Environmental Science Processes & Impacts

PAPER

View Article Online
View Journal | View Issue

Open Access Article. Published on 17 October 2019. Downloaded on 1/15/2026 12:16:42 AM.
This article is licensed under a Creative Commons Attribution 3.0 Unported Licence.

Check for updates

Cite this: *Environ. Sci.: Processes Impacts*, 2019, **21**, 2093

Using recirculating flumes and a response surface model to investigate the role of hyporheic exchange and bacterial diversity on micropollutant half-lives†

Anna Jaeger, ‡*[ab] Claudia Coll, ‡*[c] Malte Posselt,[c] Jonas Mechelke,[de] Cyrus Rutere,[f] Andrea Betterle,[dg] Muhammad Raza,[hi] Anne Mehrtens,[j] Karin Meinikmann,[a] Andrea Portmann,[k] Tanu Singh,[l] Phillip J. Blaen,[lm] Stefan Krause,[l] Marcus A. Horn,[fn] Juliane Hollender,[de] Jonathan P. Benskin,[c] Anna Sobek §[c] and Joerg Lewandowski §[ab]

Received 8th July 2019
Accepted 11th October 2019

DOI: 10.1039/c9em00327d

rsc.li/espi

Enhancing the understanding of the fate of wastewater-derived organic micropollutants in rivers is crucial to improve risk assessment, regulatory decision making and river management. Hyporheic exchange and sediment bacterial diversity are two factors gaining increasing importance as drivers for micropollutant degradation, but are complex to study in field experiments and usually ignored in laboratory tests aimed to estimate environmental half-lives. Flume mesocosms are useful to investigate micropollutant degradation processes, bridging the gap between the field and batch experiments. However, few studies have used flumes in this context. We present a novel experimental setup using 20 recirculating flumes and a response surface model to study the influence of hyporheic exchange and sediment bacterial diversity on half-lives of the anti-epileptic drug carbamazepine (CBZ) and the artificial sweetener acesulfame (ACS). The effect of bedform-induced hyporheic exchange was tested by three treatment levels differing in number of bedforms (0, 3 and 6). Three levels of sediment bacterial diversity were obtained by diluting sediment from the River Erpe in Berlin, Germany, with sand (1 : 10, 1 : 1000 and 1 : 100 000). Our results show that ACS half-lives were significantly influenced by sediment dilution and number of bedforms. Half-lives of CBZ were higher than ACS, and were significantly affected only by the sediment dilution variable, and thus by bacterial diversity. Our results show that (1) the flume-setup is a useful tool to study the fate of micropollutants in rivers, and that (2) higher hyporheic exchange and bacterial diversity in the sediment can increase the degradation of micropollutants in rivers.

Environmental significance

Contamination of rivers by wastewater-derived organic micropollutants is an emerging problem. Global-scale risk assessment and modeling, as well as regulatory decision making rely on in-depth knowledge of major factors that influence the fate of micropollutants in rivers. Sediment bacterial diversity and hyporheic exchange are parameters that are often neglected when testing persistence of substances. We present a novel experimental setup consisting of 20 recirculating flumes and a response surface model to test the influence of these two parameters on micropollutant half-lives. Our setup proved useful to study the fate of micropollutants in rivers. Our results reveal that the underrated factors, hyporheic exchange and bacterial diversity significantly affect micropollutant half-lives in rivers.

[a]*Department Ecohydrology, Leibniz-Institute of Freshwater Ecology and Inland Fisheries, Berlin, Germany*

[b]*Geography Department, Humboldt University Berlin, Berlin, Germany. E-mail: anna.jaeger@igb-berlin.de*

[c]*Department of Environmental Science and Analytical Chemistry (ACES), Stockholm University, Stockholm, Sweden. E-mail: claudia.coll@aces.su.se*

[d]*Eawag, Swiss Federal Institute of Aquatic Science and Technology, Dübendorf, Switzerland*

[e]*Institute of Biogeochemistry and Pollutant Dynamics, ETH Zürich, Zürich, Switzerland*

[f]*Department of Ecological Microbiology, University of Bayreuth, Bayreuth, Germany*

[g]*Department of ICEA and International Center for Hydrology "Dino Tonini", University of Padova, Padua, Italy*

[h]*Institute of Applied Geosciences, Technical University of Darmstadt, Darmstadt, Germany*

[i]*IWW Water Centre, Mülheim an der Ruhr, Germany*

[j]*Institute of Biology and Environmental Sciences, Carl von Ossietzky University Oldenburg, Oldenburg, Germany*

[k]*Civil and Environmental Engineering, Colorado School of Mines, Golden, Colorado, USA*

[l]*School of Geography, Earth and Environmental Sciences, University of Birmingham, Birmingham, UK*

[m]*Yorkshire Water, Bradford, UK*

[n]*Institute of Microbiology, Leibniz University of Hannover, Hannover, Germany*

† Electronic supplementary information (ESI) available. See DOI: 10.1039/c9em00327d

‡ These authors contributed equally to the publication.

§ These authors share the last authorship.

Open Access Article. Published on 17 October 2019. Downloaded on 1/15/2026 12:16:42 AM.
This article is licensed under a Creative Commons Attribution 3.0 Unported Licence.

1. Introduction

Growing consumption of pharmaceuticals and personal care products renders contamination of freshwaters by wastewater-derived trace organic micropollutants an increasing problem for aquatic ecosystems and drinking water quality.[1] Understanding the processes that determine the degradation of micropollutants in the aquatic environment is crucial to (1) better predict aquatic risks on a global scale,[2] and (2) enhance river management at a local scale to promote favorable conditions for in-stream reduction of micropollutant concentrations.[3]

Identification of key drivers of the attenuation of micropollutants in the environment has been attempted over the last few years in both field[4–7] and lab studies.[8–12] While the complex interplay of spatially heterogeneous processes and transient boundary conditions in field experiments hinders repeatability and often reduces the validity of general conclusions about mechanisms, the repeatable results obtained in lab experiments often lack diagnostic power for processes in real systems.[13] Bottle incubations carried out according to OECD guidelines 308 and 309,[14,15] for instance, are commonly used to test aerobic and anaerobic biodegradability of micropollutants in water–sediment systems. Compound specific half-lives resulting from these tests are used in current chemical legislation and for risk and exposure modeling.[2,16] However, these stagnant tests do not cover processes specific for river systems. They disregard dynamic hydrological processes, such as hyporheic exchange fluxes and the characteristics of the site-specific bacterial communities.[17–19] To this end, systematic tools that are more suitable for simulating conditions in rivers are necessary to study the fate of micropollutants.

Flumes are experimental mesocosms that can bridge the aforementioned gap between controllability of lab experiments and the authenticity of field experiments. Flumes have been proven valuable for investigating drivers of hyporheic exchange under controlled conditions[20,21] and are thus suitable to simulate hydraulic conditions in rivers. Flume designs can vary in complexity, from simple recirculating systems to those with advanced flow-control functions which can be used to simulate gaining and losing conditions in the hyporheic zone.[22] While more advanced designs are useful for testing complex hypotheses, they are clearly more challenging to replicate due to the need for additional infrastructure. In contrast, simple flume designs offer the opportunity to run experiments in parallel which enables testing of a wide range of scenarios and application of statistical models. Despite the apparent advantages of flume studies, to the best of our knowledge, there have been only a few studies investigating the fate of micropollutants in flumes. When Li *et al.*[23] and Kunkel and Radke[24] used a recirculating flume to test degradation of micropollutants, only one flume was available, which is why they repeated the experiment to test the difference between flat streambed and streambed with bedforms[23] and two different flow velocities,[24] respectively. However, no replicates and no statistical design were implemented.

Biodegradation is a key process for micropollutant transformation in rivers and is controlled by a variety of physical and biological factors. The hyporheic zone in particular represents a hot-spot of microbial activity.[25,26] It has been described as a key compartment for nutrient turnover and other biochemical reactions in rivers.[27,28] Schaper *et al.*[29] found that reach-scale removal of non-persistent polar organic micropollutants in a South Australian river was controlled by attenuation in the hyporheic zone during the wet season. Hence, enhancing the potential for hyporheic exchange will likely promote micropollutant transformation. While hyporheic flow can occur on many scales,[27] small scale exchange and short flow paths are expected to be the most effective in turnover processes.[30,31] Small scale hyporheic exchange is determined by sediment characteristics, mainly hydraulic conductivity and sediment morphology.[32] Bedforms such as dunes can induce hyporheic exchange causing a so called "pumping effect". High pressure on the upstream side of a dune forces the surface water into the sediment and low pressure on the downstream slope of the dune causes exfiltration of hyporheic water to the surface water.[20] While the extent of mass transport into the hyporheic zone and residence time distributions control the potential for turnover, the biochemical conditions control the quality of turnover. The composition of the hyporheic bacterial community is expected to play a major role in biochemical processes, but there has been little research on their impact on micropollutant degradation in rivers. Recent studies suggest that bacterial diversity in wastewater treatment plants is associated with biodegradation of certain micropollutants.[33,34] It was proposed that this positive correlation is observed when the biodegradation mechanism of a certain micropollutant can be performed by only a few bacteria taxa. There is scarce information on the compound-specific catabolic and co-metabolic pathways that are required for the biodegradation of the variety of micropollutants, and whether these are general or rare functions in bacterial communities. Stadler *et al.*[33] used a "dilution-to-extinction" approach to manipulate bacterial communities from activated sludge into different diversity levels and by this means identified taxa potentially driving the biotransformation of individual micropollutants. It was also shown that the change in taxonomic richness was associated with a change in functional richness across the treatment levels. In the absence of detailed knowledge on specific bacteria activity and functional characteristics, taxonomic diversity is a first step to understand the link between bacterial community composition and biodegradation of micropollutants.

In this study we present a novel experimental setup to test the influence of hyporheic flow and bacterial diversity on degradation half-lives of micropollutants. The experiment was based on a central composite face factorial design and used 20 flume mesocosms run in parallel to simulate different river conditions. The hyporheic flow was manipulated with the presence and number of bedforms. The bacterial diversity was controlled with a dilution-to-extinction approach.[33] The flumes were inoculated with sediment from the River Erpe in Berlin, Germany, which receives high loads of treated wastewater.[6] As the sediment of this river is continuously exposed to

 This journal is © The Royal Society of Chemistry 2019

Open Access Article. Published on 17 October 2019. Downloaded on 1/15/2026 12:16:42 AM. This article is licensed under a Creative Commons Attribution 3.0 Unported Licence.

micropollutants, its bacterial community has likely developed the capacity to degrade synthetic organic chemicals. A response surface model was used to assess the effects of the two variables (*i.e.*, sediment dilution and number of bedforms) on micropollutant dissipation half-lives (DT50s). The DT50s of the artificial sweetener acesulfame (ACS) and the anti-epileptic drug carbamazepine (CBZ) are discussed to evaluate the performance of the setup. These chemicals were chosen as model compounds due to their widespread occurrence in freshwaters, high average concentrations in River Erpe (μg L^{-1}-range)[6] and contrasting behavior in the environment. Although both compounds were previously reported as relatively persistent,[35,36] recent research found increasing degradability of ACS within the last decade, likely caused by the adaptation of microbial communities in treatment plants.[37] In addition, a study conducted in the hyporheic zone of River Erpe showed that along a vertical flow path of 40 cm, ACS was removed by 78 ± 1% while CBZ was not removed significantly.[30] Therefore, we expect generally lower half-lives and a higher influence of the tested variables for ACS than for CBZ. The study aims at: providing a new experimental method to obtain a more accurate understanding of dependencies of micropollutant half-lives on river-specific biological and physical conditions and discussing the performance of the specific experimental setup.

2. Materials and methods

2.1 Experimental design

A response surface model (RSM) and a central composite face design were employed to evaluate the effects of bacterial diversity manipulated by sediment dilution (*S*) and bedform-induced hyporheic exchange (*B*) on the attenuation of ACS and CBZ in flume mesocosms. The DT50 of ACS and CBZ in the flume system was used as a dependent variable. The two independent variables (*S* and *B*) were set at three levels (high, medium and low) as follows (Table 1):

(1) Bacterial diversity in sediment (*S*) was achieved by diluting river sediment with commercial sand in different proportions, based on the dilution-to-extinction method. In this method, the less abundant species are "removed" by stepwise dilutions, and this loss in species richness results in lower diversity.[33] The low dilution level (S1) had a sediment dilution of 1 : 10 and was expected to have the highest level of bacterial diversity, the medium level (S3) was diluted in a 1 : 10^3 ratio, and the high dilution level (S6) corresponding to the lowest expected bacterial diversity, was set to a 1 : 10^6 dilution. Bacterial diversity in S1, S3 and S6 levels was investigated through Illumina sequences of the 16S rRNA taxonomic gene (details in Chapter 2.7).

(2) Hyporheic exchange (*B*) was regulated by forming triangular-shaped stationary bedforms in the flume sediment. Bedforms cause a so-called "pumping" effect, inducing advective flow through the porous streambed by pressure differences between the upstream and downstream side of the bedform.[20] Hence, we anticipated, that higher amount of bedforms would lead to higher total exchange flux, *i.e.* the volume of water exchanged between sediment and surface water per day.[21] Consequently, the increasing solute transfer to the hyporheic zone leads to higher contact of solutes to bacterial communities and thus higher potential for micropollutant degradation in general. We aimed at creating three contrasting levels of hyporheic exchange by minimum, medium and maximum number of bedforms feasible within the present setting. Minimum exchange was expected for flat sediment (B0), followed by a medium level (3 bedforms, B3) and a high level (6 bedforms, B6). The amount of sediment was identical in all flumes and the shape of the individual bedforms was the same in the B3 and B6 flumes. The triangular shape was determined by practicality within the setting aiming at uniform shapes across flumes and inducing hyporheic exchange rather than mimicking shapes commonly found in the field. Differences in hyporheic exchange between levels B0, B3 and B6 were investigated through a salt tracer dilution test (performed at the end of the experiment) from which exchange flux, exchange volumes and average residence times were calculated (details in Chapter 2.8).

The response surface model explores non-linear effects of the bacterial diversity (*S*) and hyporheic exchange (*B*) on the dissipation half-lives (DT50s) by fitting the responses to a quadratic equation (eqn (1)):

$$\mathrm{DT50} = \beta_0 + \beta_1 S + \beta_2 B + \beta_3 SB + \beta_4 S^2 + \beta_5 B^2 + \varepsilon \qquad (1)$$

The central composite face design used here is a factorial design consisting of 20 flumes (Fig. 1a): eight flumes with the factorial variable combinations, eight flumes with axial combinations and four replicates of the center-point experiments to validate the response surface model. Central composite designs are commonly used for response surface models because they are easy to expand (*e.g.* to include more variables) and flexible in terms of choosing the values of each variable at the axial and center-points.

Table 1 Independent variables in the flume experimental design and coded values

		Coded levels		
Independent variables	Factors	−1	0	1
Hyporheic exchange – bedforms (*B*)	Level name	B0	B3	B6
	Number of bedforms	0	3	6
Bacterial diversity – sediment dilution (*S*)	Level name	S6	S3	S1
	Sediment : sand dilution ratio	1 : 10^6	1 : 10^3	1 : 10

Open Access Article. Published on 17 October 2019. Downloaded on 1/15/2026 12:16:42 AM.
This article is licensed under a Creative Commons Attribution 3.0 Unported Licence.

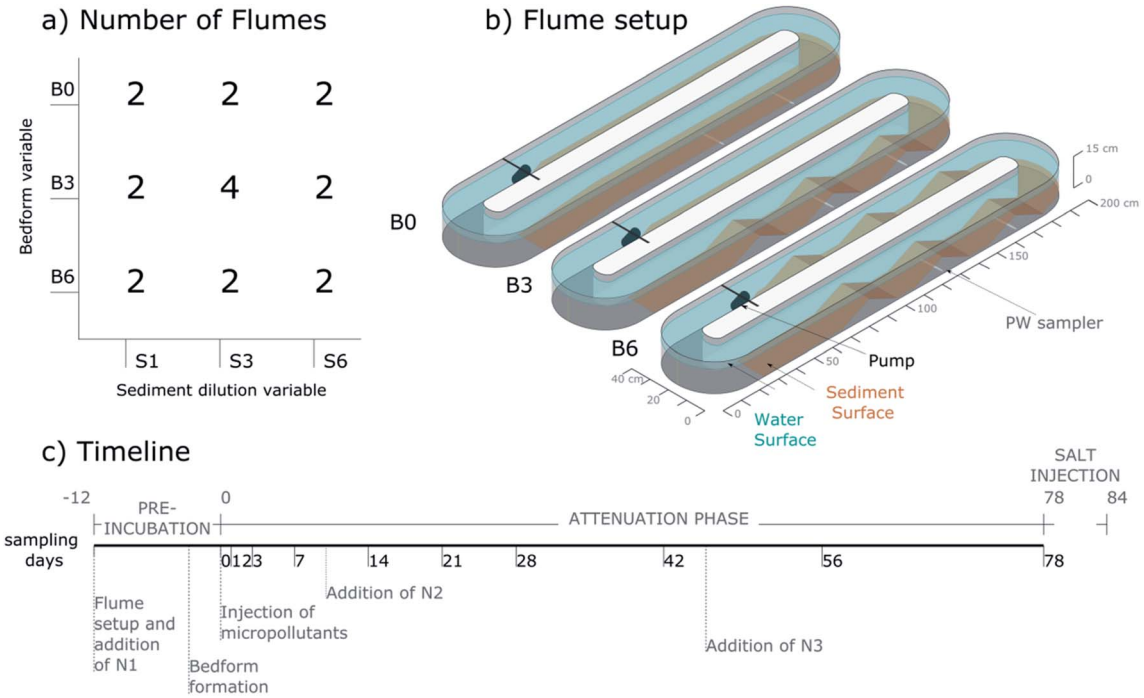

Fig. 1 (a) Number of flumes per treatment-combination (*S* and *B*) in the experimental design; (b) flume setup scheme showing the three levels of the bedform variable; (c) the timeline of the experiment indicating the days of sampling during the attenuation phase, as well as the injection times of micropollutants and the nutrient solutions (N1, N2, N3).

2.2 Preparation of the sediment-mixtures

Sediment from the River Erpe in Berlin, Germany, was collected 1 month prior to flume-setup. The sediment was homogenized and cooled at 4 °C immediately after sampling and until use. A mixture of commercial sands (Wickes, Watford, United Kingdom) was washed with tap-water to remove the finest fractions. Afterwards the sand was oven dried at 120 °C for 24 h to reduce potential microbial contamination and stored in acid-rinsed plastic barrels. The three sediment mixtures of the sediment dilution variable comprised of different ratios of sand and Erpe sediment to yield 20 L sediment for each flume (Table 2). The components of the sediment-mixtures were merged and homogenised prior to application in separate acid-rinsed containers to avoid microbial cross-contamination. The three sediment dilutions S1, S3 and S6, have similar grain size distribution, total carbon (TC), hydraulic conductivity (K_f) and porosity, as they were to at least 90% comprised of the same sand type (Table 2). Thus, the physical hydraulic characteristics across the sediment dilution levels were comparable, which was important to diminish their influence on hyporheic exchange. Any observed differences in hyporheic exchange in flumes with the same number of bedforms but different sediment dilution level should be attributable to the bacterial inocula. The influence of sediment dilution on hyporheic exchange is further discussed in Chapter 3.2.

2.3 Flume setup and pre-incubation period

The flumes were oval (2.0 m × 0.4 m), recirculating channels made of glass-reinforced plastic. The channels had an inner dimension of *ca.* 15 cm depth and 15 cm width (Fig. 1b). Prior to setup all 20 flumes were thoroughly cleaned with water, rinsed with 10% HCl and covered with plastic film until filling. The flumes were positioned inside a white tent (without floor) to shield them from weather and direct solar radiation and ensure homogenous distribution of diffuse solar radiation. However, the flumes were open to air-borne contamination from surrounding vegetation and microbes and exposed to day–night cycles of temperature. Each flume was leveled and equipped with an aquarium pump (NWA 1.6 adj 2.6 W, Newa Wave Industria, Loreggia, Italy) (see Fig. S1† for pictures of the setup procedure). Before injection of micropollutants and the start of the attenuation phase (day 0), a pre-incubation was performed to allow regrowth of the bacterial communities in diluted sediments to similar abundance (day −12 to −1; Fig. 1c). At day −12, the sediment mixtures were distributed in the flumes as shown for B0 in Fig. 1b and covered with 60 L (S1) or 58 L (S3 and S6) of deionised water (purchased from ReAgent Chemicals, Cheshire, England). The pumps were turned on simultaneously (surface water flow velocity initially *ca.* 8 cm s^{-1}). Afterwards, nutrient mix N1 (see Table S1†) was injected into the flowing water to promote the growth of the bacterial communities. Glucose was added during the pre-incubation period as carbon and energy source. On day −3, bedforms were formed by hand using custom-built wooden plates to ensure standardized bedforms of about 8 cm (bottom to crest) × 12 cm (start to crest) (Fig. S1e and f†). The plates were inserted in the flat sediment at equal distance to the position of the crest and pushed together until the desired bedform shape

 This journal is © The Royal Society of Chemistry 2019

Open Access Article. Published on 17 October 2019. Downloaded on 1/15/2026 12:16:42 AM.
This article is licensed under a Creative Commons Attribution 3.0 Unported Licence.

Table 2 Mixtures and sediment properties of the three sediment dilution levels (S1, S3, S6), the undiluted Erpe sediment and the commercial sand[a]

	S1	S3	S6	Erpe sediment	Sand
Sand base	21.3 kg sand	23.7 kg sand	23.7 kg sand	n.a.	n.a.
Inoculum	2 L Erpe sediment	Inoculum 1 (2 mL Erpe sediment in 2 L deionised water)	Inoculum 2 (2 mL inoculum 1 in 2 L deionised water)	n.a.	n.a.
TC [%]	0.007 ± 0.002	0.004 ± 0.003	0.003 ± 0.001	0.840 ± 0.066	0 ± 0
Fine gravel [%]	5	5	5	6	5
Coarse sand [%]	6	5	5	13	5
Medium sand [%]	82	83	83	68	83
Fine sand [%]	6	6	6	12	6
<0.063 mm [%]	<1	<1	<1	<1	<1
K_f at 10 °C [m s^{-1}]	$3.14 \times 10^{-4} \pm 4\%$	$3.37 \times 10^{-4} \pm 14\%$	$3.37 \times 10^{-4} \pm 14\%$	n.a.	n.a.
Porosity [%]	35	35	35	n.a.	n.a.

[a] n.a.: not applicable.

was achieved. The flat areas were leveled to about 3.5 cm sediment depth. In B6-flumes, 3 bedforms were formed on both straight sides of the flume. In B3-flumes, 3 bedforms were formed on the straight side opposite of the pump, while the side of the pump remained flat (see Fig. 1b). In the B0-flumes no bedforms were formed. During bedform formation, 10 cm porewater samplers (Standard Rhizons, Rhizosphere Research Products B.V., Wageningen, The Netherlands) were installed at 1.5 cm height in the center of the second and third bedforms (in flow direction) of B3 and B6 flumes and at equal position in the flat sediment of the B0 flumes (Fig. 1b). Three of the S1 flumes had additional porewater samplers in their first bedforms.

2.4 Injection of micropollutants and attenuation phase

After 12 days of pre-incubation and right before the addition of micropollutants, surface water and porewater samples were collected from each flume. Thereafter, the attenuation phase was started by the addition of 3 mL of methanol (Fisher Scientific UK, analytical grade) containing 31 compounds (see Table S2†) at about 200 mg L^{-1} to yield an initial concentration of 10 μg L^{-1} of each compound in each flume (day 0). The experiment ran for 78 days and samples were taken 10 times within this period (see Fig. 1c). Each set of samples was comprised of both surface water and porewater (approx. 10 mL per flume). Concentrations of micropollutants in the porewater are not discussed in the present work, but will be covered in a follow-up study. The samples were split into two aliquots and stored at −20 °C prior to micropollutant analysis at Stockholm University (SU) and the Swiss Federal Institute of Aquatic Science and Technology (Eawag), respectively. For analysis of nutrients (NO_3^-, NO_2^-, NH_4^+, PO_4^{3-} and total dissolved nitrogen) and dissolved organic carbon (DOC) the same set of porewater and surface water samples were collected on days 0, 21, 42 and 78 and surface water was sampled on the first day after the start of pre-incubation (day −12). The flumes were refilled with 3 to 5 L deionised water one time during the pre-incubation period and 5 times during the attenuation phase to account for reduction of water volume due to evaporation. Two measurements of nutrient levels during the attenuation phase revealed that dissolved nitrogen was consumed completely in the flumes of the S1 treatment. Therefore, nutrient mixtures N2 and N3 were added at days 10 and 46, respectively, to all flumes (see Table S1†). To ensure complete mixing, samples were never taken earlier than 4 days after addition of deionised water or nutrients. Flow velocities were estimated three times by recording the travel time of a floater within a set distance of the straight sides of the flumes. Two additional flumes of the S3/B3 treatment were set up (not included in the RSM), to which no micropollutants were added. They served as a control for re-mobilisation of micropollutants from the Erpe sediment to the surface water and as a control for the reaction of the bacterial community to the micropollutants. No re-mobilisation of ACS or CBZ was observed, as concentrations remained below limits of quantification (LOQ) throughout the experiment.

Open Access Article. Published on 17 October 2019. Downloaded on 1/15/2026 12:16:42 AM. This article is licensed under a Creative Commons Attribution 3.0 Unported Licence.

2.5 Boundary conditions and abiotic parameters

Inside-air and water temperature (107 probes, Campbell Scientific, Logan, UT, USA), as well as inside-solar radiation (PAR Quantum, Sky Instruments, UK) were measured in 5 min intervals during the pre-incubation period and during the first 5 weeks of the attenuation phase. Temperature and solar radiation for the remaining time of the experiment were derived from comparison of inside-values to air temperature and shortwave irradiance measured by a weather station in about 400 m distance to the experimental site (Fig. S2 and S3†). Average outside temperature during the attenuation phase was 16.3 °C (range: 7.2–30.2 °C, Fig. S2†). Outside temperature and air temperature inside the tent, as well as temperature in the flumes were correlated ($R^2 = 0.99$; coef = 0.95, $p < 0.01$, Fig. S3a and b†). The average flume water temperature during the attenuation phase was therefore also close to 16 °C. Average outside solar radiation during the attenuation phase was 261 W m^{-2} (max: 1199 W m^{-2}). Outside solar radiation [W m^{-2}] and PAR [μmol m^{-2} s^{-1}] inside the tent correlated as well ($R^2 = 0.85$; coef = 0.26; $p < 0.01$), leading to an estimated average of 68.7 μmol m^{-2} s^{-1} PAR during the attenuation phase inside the tent (Fig. S2 and S3b†).

pH in the surface water was measured two times. From day −4 to day 45, the average pH in the flumes rose from 8.1 (±0.1) to 8.5 (±0.3) (Fig. S4†). While there were no significant differences between treatments at day −4 and day 45, the sediment dilution treatment had significantly influenced pH (ANOVA; $p < 0.05$). Treatment S1 (8.2 ± 0.3) had a significantly lower pH than S3 (8.7 ± 0.1) and S6 (8.6 ± 0.2; Tukey *post hoc* test, $p < 0.05$). Dissolved oxygen (Pro 20 DO Instrument, YSI Incorporated, Yellow Springs, OH, USA) in the surface water was measured 4 times during the attenuation phase. Average O_2 saturation in all flumes ranged from 101 to 110% between days 28 and 86 (Fig. S5†). Average O_2 saturation at days 28, 36, 44 and 86 was significantly influenced by the sediment dilution treatment (ANOVA; $p < 0.05$). S1 treatments showed significantly lower O_2 saturation (103% ± 0.8) than S3 (105% ± 1.7) and S6 (106% ± 1.9; Tukey *post hoc* test, $p < 0.05$).

The method for analysis of nutrients (NO_3^-, NO_2^-, NH_4^+, PO_4^{3-} and total dissolved nitrogen) and dissolved organic carbon (DOC) is detailed in the ESI.† There was little variation in surface water nutrient dynamics between the bedform treatments, but nutrient concentrations were highly impacted by the level of sediment dilution (Fig. S6†). This is why at day 0 (injection of micropollutants), nutrient concentrations differed between sediment dilution levels. Generally the depletion of nitrogen and DOC during pre-incubation (day −12 to day 0) was higher and faster in treatments with lower dilution. Accordingly, after addition of nutrient solution N2 at day 10, removal of NH_4^+ was especially high in the lowest dilution (S1) (see ESI† for detailed discussion on nutrient dynamics).

2.6 Chemical analyses

Swiss Federal Institute of Aquatic Science and Technology (Eawag). Frozen water samples (−20 °C) were equilibrated to room temperature, which was followed by a centrifugation step (2 mL sample, 3020*g* for 30 min at 20 °C, Megafuge 1.0R, Heraeus) and the transfer of a supernatant aliquot (1 mL) into a HPLC sample vial. Isotope-labeled internal standards (IS) were directly added to the vial (20 ng mL^{-1}). The calibration series was prepared in NANOpure™ water (0, 1, 10, 100, 500, 1000, 2500, 5000 and 10 000 ng L^{-1}). Calibration standards and water samples were then injected (50 μL) into a reversed-phase C18 liquid chromatography column (Atlantis T3, 3 × 150 mm, 3 μm, Waters, USA). The samples per flume were measured in four batches and in an inverse time order (*e.g.* day 56 first and day 0 last), with blanks before and after each flume. A new calibration series was prepared and separate LOQs were calculated for every batch. Water and methanol, both acidified with 0.1% formic acid, were used as eluents for the chromatographic gradient (0% to 95% methanol in 18.5 min, 95% methanol for 10 min, 95% to 0% methanol in 4 min). The analytical column was coupled to a high-resolution tandem mass spectrometer (QExactive or QExactive Plus, Thermo Scientific, USA) by an electrospray ionization interface. Mass spectra were acquired in full-scan mode (polarity switching) at a mass resolution of 140 000 (FWHM at *m*/*z* 200) with subsequent data-dependent MS2 (Top5, mass resolution 17 500). For the quantification of target analytes, chromatographic peaks were automatically detected (5 ppm mass tolerance) and integrated (minimum three data points) using the ICIS algorithm of TraceFinder (version 4.1 EFS, Thermo Scientific, USA). Peak integrations were reviewed manually. To each target analyte (CBZ, ACS), a matching IS (ACS-D4, CBZ-D8) was assigned (internal standard method). Linear 1/*x*-weighted calibration curves were generated by fitting the analyte concentration (x) against the STD-to-IS peak area response ratio (y) without forcing the fit through zero. Nanopure water was generated with a lab water purification system (D11911, Barnstead/Thermo Scientific, USA), methanol was of LC/MS grade (Optima™, Fisher Scientific, Switzerland), and formic acid of analytical grade (≥98%, Merck, Germany). Overall, 28% of the measured samples were quality control samples (blanks, calibration standards, spike recovery samples). The LOQs of ACS were between 22 and 100 ng L^{-1} in porewater and 21 and 100 ng L^{-1} in surface water. For CBZ, LOQs were between 10 and 100 ng L^{-1}, both in porewater and surface water. The spike recovery (accuracy) was determined in porewater and surface water of flume 2 (S6/B3) after 28 days, *i.e.* approximately in the middle of the flume experiment. Spike recoveries of the two analytes were in an acceptable range, ACS was recovered at 112% and 104%, CBZ at 85% and 72%, both at high precision (RSD < 3% among duplicates) in porewater and surface water, respectively. The spike recovery test does not account for the freezing of samples but significant losses of analytes during freezing is unlikely. All samples were treated in the same way, and as the relative attenuation compared to the initial concentration is the most important parameter for this study, freezing will not have a major impact on the results.

Stockholm University (SU). Samples were analyzed using a small volume direct injection-ultra high performance liquid chromatography method coupled to tandem mass spectrometry (UHPLC-MS/MS) following a standard protocol established

Open Access Article. Published on 17 October 2019. Downloaded on 1/15/2026 12:16:42 AM. This article is licensed under a Creative Commons Attribution 3.0 Unported Licence.

previously.[38] Briefly, samples were stored at −20 degrees, defrosted at room temperature and thoroughly vortexed before processing. A sample volume of 800 μL was then combined with 195 μL methanol and the isotope-labeled internal standard mix in 5 μL methanol and after a further vortexing step filtered (Filtropur S 0.45 μm, PES membrane, Sarstedt AG&Co, Nuembrecht, Germany) into microvials (2 mL; Thermo Scientific, Dreieich, Germany). The injection volume was 20 μL. A blank sample and a quality control standard was injected every 15–20 samples. The precision determined with the quality control standard was 1.5 and 8% RSD for ACS and CBZ, respectively. In accordance with the method applied at Eawag, internal standards for ACS and CBZ were ACS-D4 and CBZ-D8. The LOQ of ACS and CBZ was 88 and 25 ng L^{-1}, respectively. Spike recoveries were in the range of 95 to 108% for ACS and 86 to 112% for CBZ. Detailed information on instrument settings, quantification and further QA/QC parameters can be found in the method section of Posselt *et al.*[38]

2.7 Bacterial diversity in sediment dilution treatments

Sediment samples (approximately 10 g per sample) were collected from each flume on day 21 of the attenuation phase and immediately frozen at −80 °C. DNA was subsequently extracted from a 0.5 g sub-sample according to the rapid protocol for the extraction of total nucleic acids from environmental samples.[39] DNA concentration was then determined with Quant-iT® PicoGreen DNA assay kit (Invitrogen, Germany). Total bacterial community was quantified based on the 16S rRNA gene using quantitative real-time PCR according to published protocols. Results from quantitative real-time PCR were used as an estimate for bacteria biomass[40,41] to evaluate the effectivity of the pre-incubation period.

Illumina Miseq amplicon sequencing targeting the 16S rRNA gene using the bacteria specific primer pair 341F and 806R was performed by LGC Genomics GmbH (Berlin, Germany) followed by post processing of the raw data as previously published.[42] Taxonomy was assigned using the Ribosomal Database Project (RDP) classifier. For comparative diversity index analyses, uneven sequencing depth among the samples was adjusted by rarefying each sample to an even sequencing depth. The sequence data were submitted to NCBI's sequence reads archive (http://www.ncbi.nlm.nih.gov/sra/) under accession no. PRJNA531245.

Fisher-alpha diversity index was calculated at a genus taxonomic level for all the samples and ANOVA was used to compare the diversity between bedform levels (B0, B3, B6) and sediment dilution levels (S1, S3, S6). Calculations were performed in the R software[43] using the vegan[44] and phyloseq[45] packages.

2.8 Salt tracer dilution test

A salt tracer dilution test was conducted at the final point of the experiment, to calculate hyporheic exchange metrics (exchange flux [L d^{-1}], exchange volume [L] and residence time [d]) in each flume.[46] After termination of the attenuation phase 50 mg NaCl were added to each flume. Flumes 11–20 were equipped with loggers (CTD-Diver, van Essen Instruments, Delft, the Netherlands) for electrical conductivity (EC), while in flumes 1–10 EC was monitored using a hand-hold EC-meter. The recessions of the electrical conductivity resulting from the dilution of NaCl were measured for 163 hours. The electrical conductivity of the surface water will be diluted as a consequence of hyporheic exchange, as surface water with high salt concentration will gradually mix with porewater of lower salt concentration. To account for deviations between devices, all loggers and the manual EC-meter were calibrated relative to one of the loggers, using five NaCl solutions of different concentrations. The EC values were then corrected by the calibration curves of the single loggers. Details on the calculation of hyporheic exchange metrics can be found in the ESI.†

2.9 Dissipation half-lives and response surface model

The concentrations of ACS and CBZ (C_x in eqn (2a)) were first divided by the respective measured initial concentration at day 1 (C_0 in eqn (2a)) to scale time trends from 0 to 1. Concentrations below LOQ in both data sets were excluded. Normalized concentrations measured in Eawag and SU have a good agreement with an average RSD of 7.9% for CBZ and 6.8% for ACS (Fig. 2). Eawag and SU data sets were therefore pooled and averaged for all the individual timepoints. Measurements that were available in only one data set (*e.g.* concentrations at days 2 and 78 were only available in the SU data set) were used directly in the analysis (Fig. 2).

The DT50s for CBZ and ACS were calculated assuming first order kinetics by fitting the timepoint-averaged measured concentrations to an exponential function (eqn (2a) and (2b)). If no dissipation was observed in the initial timepoints, this period was considered as lag-phase and was excluded from the DT50 calculation.

$$C_x = C_0 e^{-k_{dis}t} \tag{2a}$$

$$DT50 = -\ln(2)/k_{dis} \tag{2b}$$

The goodness of fit of the first-order dissipation assumption was assessed with a one-tailed *t*-test of the kinetic constants (k_{dis}) to be significantly different from zero. Only DT50s obtained from kinetic constants (k_{dis}) significantly different from zero ($p \leq 0.05$), $n = 20$ for ACS and $n = 18$ for CBZ, were fitted to a quadratic response surface model (RSM; eqn (1)), using the rsm package (Lenth RV, 2009) in the R software.[43]

The coded levels (−1, 0 and 1) were used for the sediment dilution (S) and bedform (B) variables (Table 1). The use of the coded variables to fit the RSM is adequate for our specific goal to understand the relative size and effect of the variables, as in the present study we do not aim to predict the DT50s or optimize the attenuation of micropollutants. The model coefficients β_x (eqn (1)) were first calculated using ordinary least squares, then tested to be significantly different from zero (two-tailed *t*-test), and finally an analysis of variance (ANOVA) was used to evaluate the significance of the first (β_1 and β_2), second order (β_4 and β_5) and interaction (β_3) terms. The adjusted-R^2, *F*-test and model lack-of-fit were calculated to assess goodness of fit and adequacy of the regression.

Open Access Article. Published on 17 October 2019. Downloaded on 1/15/2026 12:16:42 AM.
This article is licensed under a Creative Commons Attribution 3.0 Unported Licence.

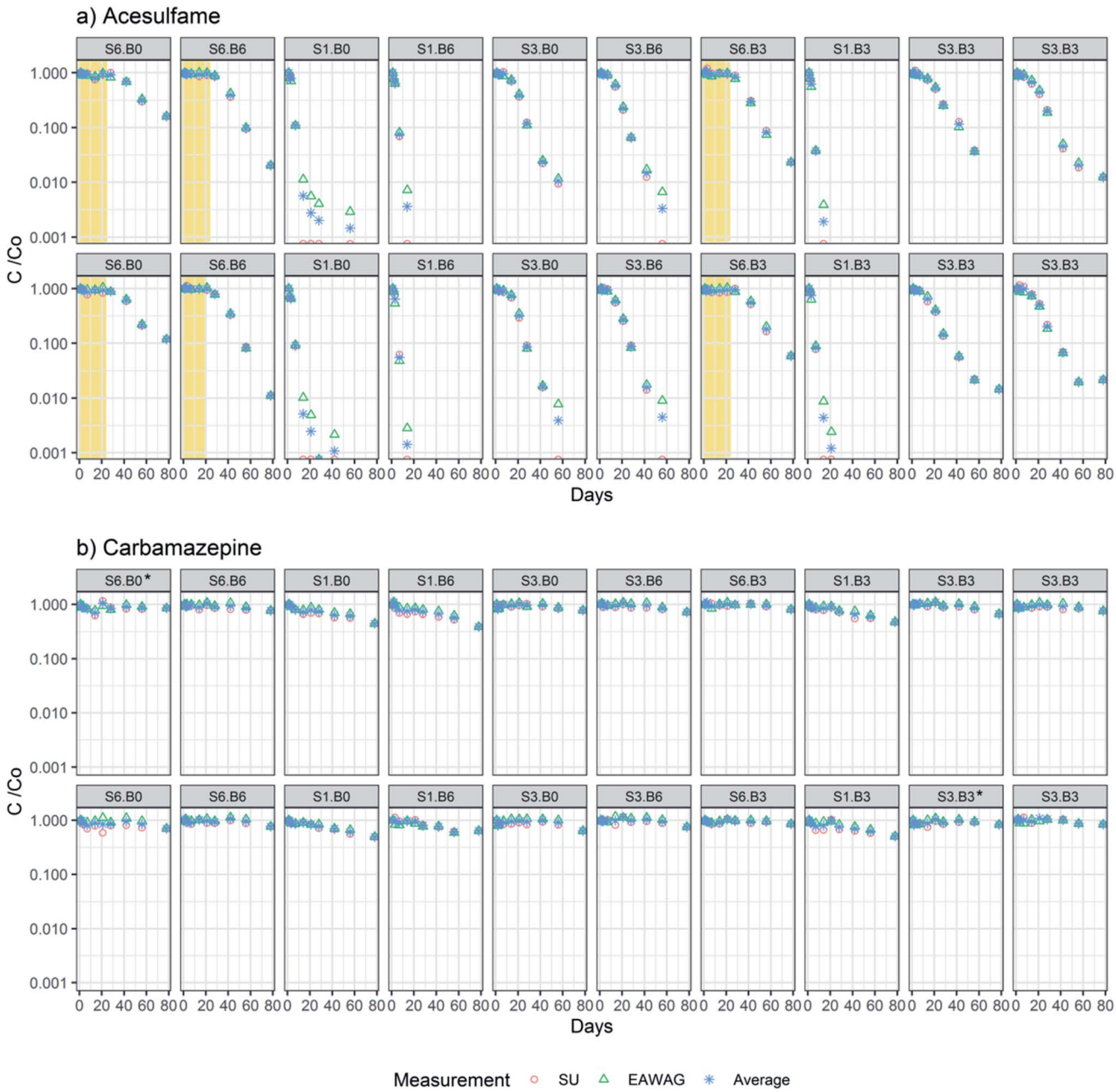

Fig. 2 Normalized concentrations (C/C_0) of (a) acesulfame and (b) carbamazepine, plotted per flume, as measured in SU and EAWAG. The average normalized concentration per time point (blue stars) were used to fit the first order dissipation kinetics. The sediment dilution level (S1, S3 or S6) and bedform level (B0, B3, B6) are indicated for each flume. The concentration plots of ACS in flumes corresponding to the high sediment dilution (S6) show a clear lag-phase of 21–28 days (in yellow) in which no dissipation can be observed, followed by a period of degradation. Flumes marked with * could not be fitted to 1st order kinetics. Note the *y*-axis is in log-scale.

3. Results and discussion

3.1 Effect of sediment dilution and bedforms on bacterial diversity

The sediment dilution caused a significant decrease in bacterial diversity (based on the Fisher's alpha index) observed in the flume sediment at day 21 (ANOVA; $p \leq 0.01$, Fig. 3b), whereas no significant effects on diversity were observed for the bedform variable or the interaction term (Fig. 3a). Hence, the sediment dilution used in our study based on the "dilution-to-extinction" method[33] effectively induced different bacterial diversity levels in the flume sediments.

Although the combination of medium sediment dilution and medium bedform number (S3 : B3) had slightly higher average bacterial diversity than the other medium dilution (S3) samples (S3 : B0 and S3 : B6), this difference was not significant in a Tukey *post hoc* analysis. The overall difference in Fisher's alpha bacterial diversity was less pronounced between medium

 This journal is © The Royal Society of Chemistry 2019

Open Access Article. Published on 17 October 2019. Downloaded on 1/15/2026 12:16:42 AM.
This article is licensed under a Creative Commons Attribution 3.0 Unported Licence.

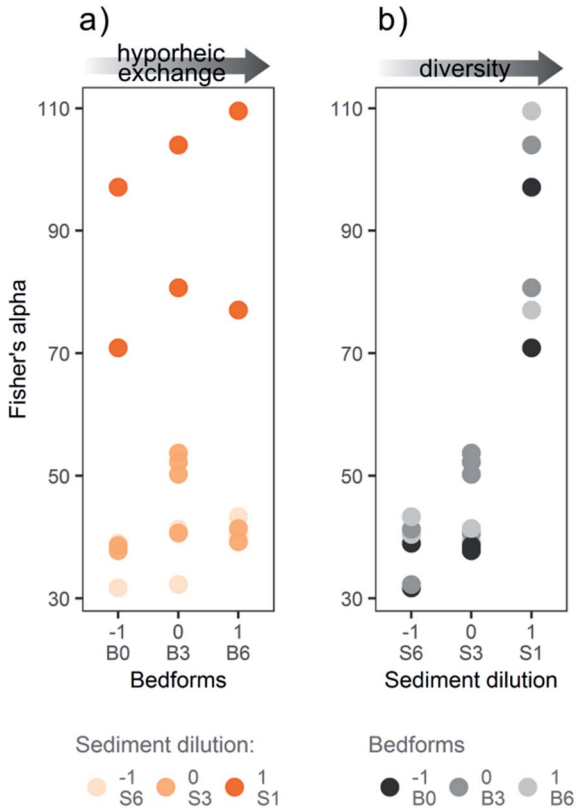

Fig. 3 Fisher's alpha diversity index at day 21 plotted by (a) bedform and (b) sediment dilution levels. The bacterial diversity was significantly different between the sediment dilutions ($p \leq 0.01$), whereas the bedform variable did not significantly affect the diversity.

and high sediment dilution levels (S3 and S6) than between low and medium dilutions (S1 and S3, Fig. 3b). Since Fisher's alpha index gives more weight to the total number of species, and less to the number of individuals in each species,[47] the medium and high dilutions (S3 and S6) were similar in taxonomic richness, but the bacterial community composition could still be considerably different. The dispersion of the Fisher's alpha index differed between the sediment dilution levels: the low dilution (S1) had the widest range in values (RSD 18%), followed by the medium dilution (S3; RSD 15%) and finally the high dilution (S6; RSD 13%). Due to the extinction effect, the communities in the low dilution flumes (S1) evolved from the original heterogeneity of river sediment causing a wider spread of diversities, while the communities in the medium and high dilution flumes (S3 and S6) evolved from inocula with similar pre-selected bacterial communities with lower taxonomic richness.

Due to the dilution-to-extinction method, the number of bacterial cells at the start of pre-incubation (day −12) and corresponding number of copies of the 16S rRNA gene, was theoretically lower in the medium and high sediment dilutions (S3 and S6) compared to the low dilution (S1). This was not the case anymore at day 21. Sediment treatments at day 21, obtained an average of 4.7×10^5 copies of the 16S rRNA gene per gram of sediment dry weight after real-time PCR (Fig. S8†) and were not significantly different between the sediment dilution levels (ANOVA; $p > 0.05$). Further, there was no significant effect of the bedform variable on the copy numbers of 16S rRNA gene (ANOVA; $p > 0.05$). Thus, substantial bacterial growth in the high dilutions (S3 and S6) was necessary during the pre-incubation phase to reach a similar number of copies to the low dilution (S1) at day 21, suggesting that the pre-incubation was successful. This reveals that the main effect of the sediment dilution was likely caused by differences in bacterial diversity, and not differences in biomass. Still, it should be pointed out that the copy numbers of 16S rRNA genes do not necessarily correlate to bacterial biomass or number of bacteria.[48] First, because the number of copies of the 16S rRNA gene in the chromosome is taxon specific (from 1 to more than 10). Second, because the 16S rRNA gene copy number for a specific taxon can differ between growth phases. Our results for bacterial diversity and 16S rRNA gene copies show the status of bacterial communities in the flumes at day 21, which is representative of the period where most micropollutant attenuation occurred, yet it is possible that the communities evolved over the duration of the test and in response to environmental conditions such as sunlight, temperature and addition of nutrients.

3.2 Effect of sediment dilution and bedforms on hyporheic exchange

We aimed to quantify differences in surface water − porewater exchange flux [L d^{-1}] and exchange volume [L], as well as average residence time [d] between bedform levels by the salt-tracer dilution test[46] after termination of the attenuation phase (ESI†).

The test showed that the sediment dilution-variable significantly influenced the exchange flux (ANOVA; $p < 0.05$), while the bedform-variable had no significant effect at this late point in time. Neither the bedform, nor the sediment dilution variable influenced the exchange volume or the residence time significantly (Fig. S7†). In contrast to what we found, we expected that an increasing number of bedforms would induce higher hyporheic exchange due to advective pumping[20] and this way increase contact of micropollutants to hotspots of favorable turnover conditions. Previous studies have found differences in hyporheic exchange in flumes with flat beds and in flumes with bedforms, containing the same sediment.[21]

We attribute the lack of significant effect of bedforms on exchange parameters to the fact that the salt-tracer dilution test was conducted at the final point of the experiment (days 78–84), a time by which the flumes had changed from their initial setup conditions (Table 3). Formation of biofilms and algae and settling of fine particulate matter, more pronounced at the end of the test, likely influenced the permeability of the sediment by clogging and affected hyporheic exchange. Bedform heights had dropped by 19% compared to the beginning of the setup due to gradual erosion, potentially reducing exchange flux in B3 and B6 treatments (Table 3). Small ripples had formed in the flumes without bedforms caused by turbulence in the flume curves, which likely increased the exchange flow in the B0

Open Access Article. Published on 17 October 2019. Downloaded on 1/15/2026 12:16:42 AM. This article is licensed under a Creative Commons Attribution 3.0 Unported Licence.

Table 3 Average change in morphology of all bedforms and surface water velocities in all flumes. A detailed version of this table is presented in the ESI (Table S3)[a]

Day of measurement	−3	27	46	82	Reduction by day 27	Reduction by day 46	Reduction by day 82
Height of the bedforms [cm]	8	7.8 ± 0.8	7.3 ± 0.8	6.5 ± 0.9	3%	9%	19%
Depth valleys [cm]	2	n.m.	1.94	1.84		3%	8%
Water level from bottom [cm]	12	11.5 ± 0.4	11.7 ± 0.4	11.2 ± 0.5	4%	3%	7%
Surface water velocity bedforms [cm s^{-1}]	n.m.	8.2 ± 1.2	8.3 ± 1.1	6.6 ± 1.8		−1%	19%
Sediment depth flat [cm]	3.5	3.8 ± 0.3	3.7 ± 0.2	3.4 ± 0.2	−9%	−6%	3%
Surface water velocity flat [cm s^{-1}]	n.m.	9.2 ± 1.7	10.3 ± 1.4	7.4 ± 2.2		−11%	20%

[a] n.m.: not measured.

treatments over time. The average flow velocity had decreased by 19% from initial bedform setup (day −3) to day 82 due to decreasing pump performance (Table 3). Differences in flow velocity might also have contributed to the effect of the sediment dilution treatment on the exchange flux at the time of the salt tracer test. By then, S1 treatments had the lowest average flow velocity (6.1 cm s^{-1}), followed by S3 treatments (6.8 cm s^{-1}) and S6 treatments (7.9 cm s^{-1}), although these differences were not significant (ANOVA; $p > 0.05$). The lower flow velocities in S1 flumes might have been caused by clogging of the pumps due to floating algae, which appeared in the second half of the attenuation phase in S1 flumes (Fig. S10†).

While the salt tracer dilution test showed that hyporheic exchange did not differ between bedform treatments at the final point of the experiment, it can not be ruled out that the bedforms caused differences in hyporheic exchange as anticipated in the beginning of the experiment and most relevant time for degradation (Fig. 2a). Hydrodynamic modelling could be used to calculate bedform-induced hyporheic exchange under initial setup conditions in the different bedform treatments.[49,50] However, this was outside the scope of the present study. A follow-up study will cover this endeavor.

3.3 Response surface model to evaluate dissipation of acesulfame and carbamazepine

We observed dissipation of both ACS and CBZ in the flumes. ACS was dissipated by 83–99% in S6 flumes, by 97–100% in S3 flumes and 100% in all S1 flumes, at day 78. A lag-phase period of around 20 days in the attenuation of ACS can be clearly identified in flumes with S6 sediment (highest dilution level) (Fig. 2a). The lag phase can be interpreted as the time it takes for the bacterial community to adapt to transform ACS, as the bacteria with that function may originally have been less abundant in sediment S6. The DT50s of ACS were between 2.1 and 36 days (Fig. 4a and b), and all flumes had a kinetic constant significantly different from zero. In contrast, the concentrations of CBZ in flume surface water had decreased by 37–61% in S1 treatments at day 78, and a smaller decrease was observed in flumes with S3 treatment (16–36% removal) and S6 levels (14–30% removal). The DT50s of CBZ ranged between 65 and 838 days (Fig. 4d and e). The concentrations of CBZ over time in two of the flumes (treatments S6 : B0 and S3 : B3) could not be fitted to 1st order kinetics because no discernable attenuation was observed (Fig. 2b). DT50s of those flumes were not included in further analysis nor in Fig. 4d and e. Of the 18 DT50s obtained for CBZ, 6 had kinetic constants that were not significantly different from zero ($p > 0.05$) and 70% of the DT50s calculated for CBZ exceeded the 120 day persistence criteria for sediment in the REACH regulation.[51]

ACS and CBZ were ubiquitously found in a field study in River Erpe, the river from which the sediment was collected for the flumes, with surface water concentrations in the μg L^{-1}-range and both compounds were more persistent relative to other micropollutants.[6] While DT50s of ACS observed in the River Erpe were in the same order of magnitude (4–30 days) as the DT50s in our flume setup, the *in situ* DT50s of CBZ were about one order of magnitude lower (4–13 days) compared to in our flumes. Also, Writer *et al.*[52] observed lower DT50s of CBZ of 21.0 ± 4.5 h in a small creek in Colorado and Acuña *et al.*[53] found CBZ DT50s of 4.1 ± 2.4 h in rivers in Spain. On the other hand, a previous flume experiment[23] showed infinite DT50s of CBZ. Three *in situ* studies that tested ACS and CBZ found poor to no degradation of both compounds.[5,29,54] The variability in literature values of DT50s for both ACS and CBZ reflect the complex interactions between dissipation processes and environmental conditions that in turn may influence degradation rates.

The RSM of ACS explained roughly 90% of the variance of observed DT50s (adjusted-R^2 of 90.2%) and the overall model was significant, meaning that the coefficients together fitted the DT50s better than just the mean (F-statistic: 35.79 on 5 and 14 degrees of freedom, $p \leq 0.05$, see Table 4 and Fig. 4c). The ANOVA showed that both first, second order and interaction terms were significant for the RSM. However, the lack of fit of the model was also significant, which means that the difference between the model predictions and the average of measurements for each variable combination (S1 : B0, S3 : B0, S6 : B0, *etc.*) was large compared to the pure error that was expected due to chance. The difference between predicted *vs.* observed DT50s was higher in S3 and S6 levels, which also have the highest variations in DT50s (Fig. 4b). Therefore, variation in the DT50s was not adequately explained by the variables S and B in the ACS-RSM. The CBZ-RSM was found significant and had an adjusted-R^2 of 44.4% (Table 4 and Fig. 4f). Only the linear term of the model was significant for the fit and thus the quadratic terms were not significantly improving the model performance.

Open Access Article. Published on 17 October 2019. Downloaded on 1/15/2026 12:16:42 AM.
This article is licensed under a Creative Commons Attribution 3.0 Unported Licence.

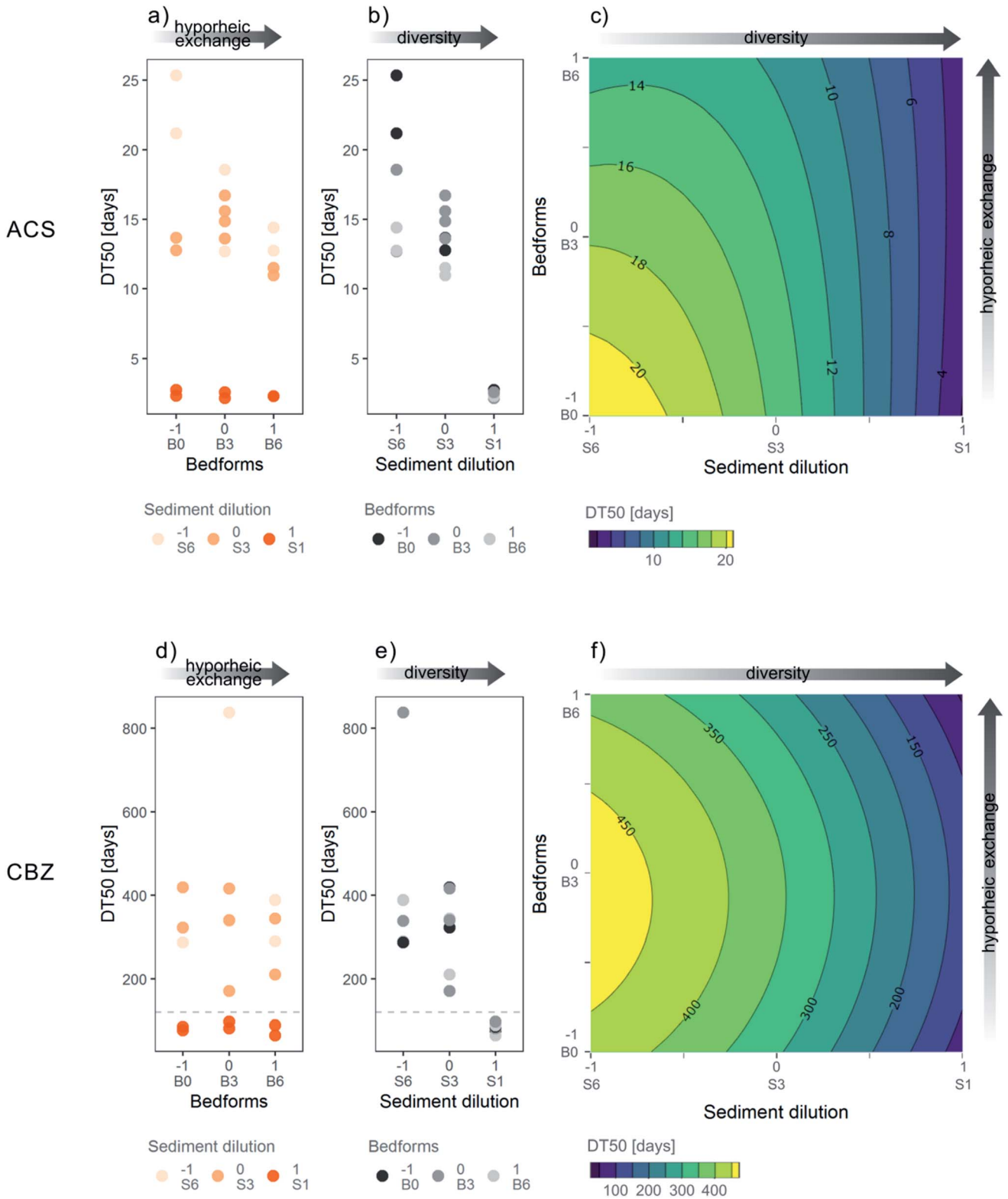

Fig. 4 Dissipation half-lives (DT50s) of (a–c) acesulfame (ACS) and (d–f) carbamazepine (CBZ) in the 20 flumes included in the central composite face design. The three levels in the variable bedform correspond to −1 = flat, 0 = 3 bedforms, 1 = 6 bedforms, and for sediment dilution −1 = 1 : 10^6, 0 = 1 : 10^3, 1 = 1 : 10. To the right is a contour plot of the response surface model fitted for (c) ACS and (f) CBZ. The grey dotted horizontal line in CBZ plots (d and e) represents the 120 day persistence criteria for sediment.

Open Access Article. Published on 17 October 2019. Downloaded on 1/15/2026 12:16:42 AM. This article is licensed under a Creative Commons Attribution 3.0 Unported Licence.

Table 4 Response surface model (RSM) coefficients fitted to a quadratic equation and p-value, and the ANOVA of each model component (first, second order, and interaction terms) for the sediment dilution (S) and bedform (B) variables. The coefficients β_1 and β_2 correspond to the linear effects of the S and B variables respectively, β_3 to the interaction term SB and β_4 and β_5 to the quadratic effects S^2 and B^2 (see eqn (1))[a]

	Acesulfame		Carbamazepine	
	Coefficient	p-Value	Coefficient	p-Value
RSM parameters				
Intercept – (β_0)	13.95	4.30×10^{-10}*	357.72	1.78×10^{-4}*
Linear term – S (β_1)	−7.55	9.05×10^{-9}*	−172.78	0.002*
Linear term – B (β_2)	−1.99	0.007*	−19.18	0.671
Interaction term – SB (β_3)	2.36	0.008*	3.53	0.950
Quadratic term – S^2 (β_4)	−3.70	0.002*	−55.58	0.440
Quadratic term – B^2 (β_5)	−0.46	0.653	−70.49	0.331
Adjusted-R^2		0.902		0.444
Model p-value		1.71×10^{-7}*		0.029*
RSM ANOVA				
First order (β_1 and β_2)		2.7×10^{-8}*		0.005*
Second order (β_4 and β_5)		0.007*		0.442
Interaction (β_3)		0.008*		0.826
Lack of fit		0.048*		0.364

[a] * indicates significance at the 0.05 level.

The overall interpretation of the CBZ-RSM model is that only the sediment dilution variable (S) was a good explanatory variable of the DT50s of CBZ in our flume set-up.

The main removal process of ACS and CBZ in this experiment was expected to be biodegradation. Although CBZ was often found persistent and thus not biodegradable in sediment–water systems,[8,13,23,55] in experiments comprising longer incubation times, slow biodegradation has been observed previously.[9,56–58] Biodegradation of ACS in WWTPs was only recently reported and has evolved either by independent evolution or global spreading of organisms or genes responsible for the biotransformation pathway.[37] Bacteria in sediment of River Erpe have been chronically exposed to ACS *via* the effluent of the local WWTP and could have developed the capability to degrade ACS similar to the WWTP communities. Neither photolysis nor hydrolysis has been relevant for ACS and CBZ attenuation in previous studies.[8,59]

Sorption is expected to influence the dissipation from water for compounds with high log K_{OW} as they sorb to hydrophobic fractions of organic matter, or for positively charged compounds due to electrostatic interactions with negatively charged binding sites of clay minerals, biofilm or organic matter.[52,60,61] Low sorption potential of ACS is expected, as ACS is negatively charged at ambient pH of around 8 and has a log K_{OW} of −0.6. Accordingly, previous studies showed low sorption[62] and a low retardation coefficient (max. 1.2)[30] in sediments. All flume sediments had low organic carbon content (TC < 0.01%) and low content of fine particles (silt + clay < 1%), which generally rendered them poor sorbents. CBZ is neutral, has a log K_{OW} of 2.77, and has been shown to sorb to organic matter[63] and to have relatively high retardation coefficient in sediment (3.6).[30] However, a test following OECD guideline 106 [64] to examine potential sorption of CBZ to the flume sediments showed no sorption of CBZ to S1, S3 or S6 sediments (see ESI for details, Fig. S11 and S12†). This can be explained mainly by the low carbon content of the flume sediments. Therefore, sorption was not a relevant attenuation process of CBZ or ACS in our experimental setup.

3.4 Impact of sediment dilution treatments on dissipation half-lives of acesulfame and carbamazepine

The level of sediment dilution, and hence the bacterial diversity, had a significant influence on the dissipation of ACS and CBZ in our flume experimental setup. ACS had significant linear and quadratic coefficients (Table 4) of the sediment dilution variable (S). Both coefficients were negative and indicate that faster degradation was observed in flumes with the lowest sediment dilution (S1), *i.e.* flumes with the highest bacterial diversity (Fig. 4b). The CBZ model had the linear term of the sediment dilution (S) significant and negative, which conveys that the sediment dilution had an effect on the DT50s and the lower sediment dilution (S1) generated shorter DT50s (Table 4, Fig. 4e).

Manipulating the bacterial community without changing chemical and physical background conditions was challenging. The difference in pH (∼0.5) and O_2 (∼3%) in the low dilution (S1) compared to the medium and high levels (S3 and S6) was significant, but likely too low to influence the degradation of micropollutants considerably. In contrast, the differences in nutrient concentrations and nutrient depletion over time were high between the different sediment dilution treatments (Fig. S6†). The low sediment dilution level (S1) had the highest depletion of nutrients and lower long-term availability of nutrients for bacteria. Hence, DT50s decreased in the lower sediment dilution although nutrient concentrations were lower. Thus, the deficiencies in nutrient concentrations could have counteracted the positive effect of the high bacterial diversity in S1 which implies that the effect of the sediment dilution on

Open Access Article. Published on 17 October 2019. Downloaded on 1/15/2026 12:16:42 AM.
This article is licensed under a Creative Commons Attribution 3.0 Unported Licence.

DT50s of ACS and CBZ might have been even higher at equal nutrient availabilities. Therefore, despite some differences in chemical conditions, the significant influence of sediment dilution levels on degradation of ACS and CBZ can be attributed to the differences in bacterial diversity. A positive association between biodegradation rates and biodiversity has been reported for bacteria in WWTPs.[33,34] The faster dissipation of ACS and CBZ in sediment with the highest diversity (S1) is consistent with a mechanism referred to as "sampling effect". Briefly, if the biodegradation of a micropollutant is a rare function performed by few bacteria species, which is likely for slowly degrading compounds, the bacteria capable of degrading these compounds are more likely found in sediment with the highest bacterial diversity. In addition, the "complementarity effect", meaning that higher diversity leads to higher functionality and more cooperating specialist strains, might increase complexity and efficiency in transformation pathways of particular micropollutants.[65] The "sampling" and "complementarity" effects can be applied also to describe the increasing variability of DT50s of ACS in the higher sediment dilutions (S3 and S6): key species necessary for the efficient degradation of ACS are less likely to be present or randomly found in bacteria communities with low diversity. The variation in bacterial communities in the sediment dilutions thus might be responsible for the lack of fit of the RSM of ACS.

3.5 Impact of bedform treatments on dissipation half-lives of ACS and CBZ

The presence of bedforms increased degradation of ACS as the linear coefficient for the bedform variable (B) was significant and negative for ACS (Fig. 4a and Table 4). This indicates that despite no measurable differences in exchange at the end of the experiment, at times most relevant for ACS degradation, the bedform treatment induced different levels of hyporheic exchange as hypothesized. The redox-sensitivity of ACS might have contributed to the finding of this effect in contrast to CBZ.[66,67] In addition to more intense transport, hyporheic exchange results in altered redox zonation along the flow paths, primarily by transport of dissolved oxygen into the sediment.[68,69] ACS was previously reported to degrade effectively under oxic and denitrifying conditions[66] and in the hyporheic zone.[30] Therefore, higher presence of bedforms results in better degradation of ACS by increasing the transport of ACS into the hyporheic zone and by providing qualitatively favorable redox conditions for ACS degradation.

The coefficients in the RSM showed that the effect of the bedform variable (B) on the DT50s was smaller than the effect of the sediment dilution (S) and the interaction between the two variables (S and B), was significant and positive for ACS (Table 4, Fig. 4a). Therefore, the combination of high sediment dilution (low bacterial diversity) and absence of bedforms (low hyporheic exchange), had a negative effect on the attenuation of ACS and resulted in longer DT50s (Fig. 4c). The significant interaction between sediment dilution and bedform also implies that the effect of bedform treatment was higher at higher sediment dilution (Fig. 4c), indicating that the strong impact of high diversity on the dissipation rate of ACS in the low dilution treatment might have covered the effect of the bedform variable.

For CBZ, no effect of bedforms on dissipation rates could be shown, because the coefficients in the RSM of the bedform variable (B) and the interaction coefficient were not significant ($p > 0.05$, Table 4, Fig. 4d). In two of the flumes, one from level B0 and one from B3, it was not possible to calculate DT50s, and they were excluded from the RSM calculations. The absence of these two potentially long DT50s could have additionally masked an effect of the bedform variable. Given the generally slow degradation of CBZ, the effect of the bedform levels might have been too low to be detectable in the present setup.

4. Conclusion

We showed that this elaborate flume setup can be used to study the degradation of micropollutants under more natural conditions than batch experiments without having to sacrifice the repeatability and control over test conditions. Our experimental design highlights the importance of hyporheic exchange, as higher number of bedforms can significantly increase the attenuation of particular micropollutants, as shown for ACS in the present case. Furthermore, our results reveal that bacterial diversity of river sediment has a paramount effect on the degradation of micropollutants. This particularly shines new light on the interpretation of DT50s in literature, which have been obtained from various experimental setups in which the composition of the bacterial communities have usually been ignored.

In the future, the setup we presented can be applied to other parameters that influence degradability, for instance sediment properties, nutrient concentrations or plant cover. For future studies, we suggest a set of preliminary studies or modelling to test the suitability of appropriate treatment levels for all variables tested. For instance, higher effects of and differences in hyporheic exchange can be ensured by preliminary hydrodynamic modeling of bedform morphologies. A second important improvement would be the continuous monitoring of chemical parameters to maintain comparable nutrient and chemical conditions. We used coded variable levels to investigate the suitability of the experimental design, but future studies could enhance the use of this design to quantify the effect of variables on DT50s of micropollutants.

The use of a central composite face design to fit a response surface model provides a robust statistical method to study the response of micropollutant attenuation to certain environmental drivers and highlight bacterial diversity as a disregarded factor in testing persistence of micropollutants. To the best of our knowledge, no other flume study includes a full experimental design with replicates. This study guides a way forward for more elaborate experimental setups that address how environmental processes affect the fate of micropollutants in rivers.

Conflicts of interest

The authors declare no conflicts of interest.

Open Access Article. Published on 17 October 2019. Downloaded on 1/15/2026 12:16:42 AM.
This article is licensed under a Creative Commons Attribution 3.0 Unported Licence.

Acknowledgements

The work has received funding from the European Union's Horizon 2020 research and innovation programme under Marie Sklodowska-Curie grant agreement No. 641939 and additionally from the Research Training Group 'Urban Water Interfaces (UWI)' (GRK 2032/1) funded by the German Research Foundation (DFG). We thank Ignacio Peralta-Maraver, Sheelajini Paramjothy, Jason Galloway, Grit Siegert, Torsten Preuer and Christine Sturm for their support in the experimental work.

References

1 T. aus der Beek, F. A. Weber, A. Bergmann, S. Hickmann, I. Ebert, A. Hein and A. Kuster, Pharmaceuticals in the environment–Global occurrences and perspectives, *Environ. Toxicol. Chem.*, 2016, **35**(4), 823–835.

2 R. Oldenkamp, A. H. W. Beusen and M. A. J. Huijbregts, Aquatic risks from human pharmaceuticals—modelling temporal trends of carbamazepine and ciprofloxacin at the global scale, *Environ. Res. Lett.*, 2019, **14**(3), 034003.

3 K. T. Peter, S. Herzog, Z. Tian, C. Wu, J. E. McCray, K. Lynch and E. P. Kolodziej, Evaluating emerging organic contaminant removal in an engineered hyporheic zone using high resolution mass spectrometry, *Water Res.*, 2019, **150**, 140–152.

4 U. Kunkel and M. Radke, Fate of pharmaceuticals in rivers: Deriving a benchmark dataset at favorable attenuation conditions, *Water Res.*, 2012, **46**(17), 5551–5565.

5 G. Guillet, J. L. A. Knapp, S. Merel, O. A. Cirpka, P. Grathwohl, C. Zwiener and M. Schwientek, Fate of wastewater contaminants in rivers: Using conservative-tracer based transfer functions to assess reactive transport, *Sci. Total Environ.*, 2019, **656**, 1250–1260.

6 A. Jaeger, M. Posselt, A. Betterle, J. Schaper, J. Mechelke, C. Coll and J. Lewandowski, Spatial and Temporal Variability in Attenuation of Polar Organic Micropollutants in an Urban Lowland Stream, *Environ. Sci. Technol.*, 2019, **53**(5), 2383–2395.

7 J. L. Schaper, W. Seher, G. Nutzmann, A. Putschew, M. Jekel and J. Lewandowski, The fate of polar trace organic compounds in the hyporheic zone, *Water Res.*, 2018, **140**, 158–166.

8 R. M. Baena-Nogueras, E. González-Mazo and P. A. Lara-Martín, Degradation kinetics of pharmaceuticals and personal care products in surface waters: photolysis *vs.* biodegradation, *Sci. Total Environ.*, 2017, **590–591**, 643–654.

9 Z. Li, M. P. Maier and M. Radke, Screening for pharmaceutical transformation products formed in river sediment by combining ultrahigh performance liquid chromatography/high resolution mass spectrometry with a rapid data-processing method, *Anal. Chim. Acta*, 2014, **810**, 61–70.

10 N. Schmidt, D. Page and A. Tiehm, Biodegradation of pharmaceuticals and endocrine disruptors with oxygen, nitrate, manganese(IV), iron(III) and sulfate as electron acceptors, *J. Contam. Hydrol.*, 2017, **203**, 62–69.

11 Y. F. Velázquez and P. M. Nacheva, Biodegradability of fluoxetine, mefenamic acid, and metoprolol using different microbial consortiums, *Environ. Sci. Pollut. Res.*, 2017, **24**(7), 6779–6793.

12 K. Nodler, M. Tsakiri and T. Licha, The impact of different proportions of a treated effluent on the biotransformation of selected micro-contaminants in river water microcosms, *Int. J. Environ. Res. Public Health*, 2014, **11**(10), 10390–10405.

13 M. Radke and M. P. Maier, Lessons learned from water/sediment-testing of pharmaceuticals, *Water Res.*, 2014, **55**, 63–73.

14 OECD, Test No. 308, *Aerobic and Anaerobic Transformation in Aquatic Sediment Systems*, 2002.

15 OECD, Test No. 309, *Aerobic Mineralisation in Surface Water – Simulation Biodegradation Test*, 2004.

16 M. Honti and K. Fenner, Deriving persistence indicators from regulatory water-sediment studies–Opportunities and limitations in OECD 308 data, *Environ. Sci. Technol.*, 2015, **49**(10), 5879–5886.

17 M. Honti, S. Hahn, D. Hennecke, T. Junker, P. Shrestha and K. Fenner, Bridging across OECD 308 and 309 Data in Search of a Robust Biotransformation Indicator, *Environ. Sci. Technol.*, 2016, **50**(13), 6865–6872.

18 M. Honti, F. Bischoff, A. Moser, C. Stamm, S. Baranya and K. Fenner, Relating Degradation of Pharmaceutical Active Ingredients in a Stream Network to Degradation in Water-Sediment Simulation Tests, *Water Resour. Res.*, 2018, **54**(11), 9207–9223.

19 P. Shrestha, T. Junker, K. Fenner, S. Hahn, M. Honti, R. Bakkour, C. Diaz and D. Hennecke, Simulation Studies to Explore Biodegradation in Water–Sediment Systems: From OECD 308 to OECD 309, *Environ. Sci. Technol.*, 2016, **50**(13), 6856–6864.

20 A. H. Elliott and N. H. Brooks, Transfer of nonsorbing solutes to a streambed with bed forms: Theory, *Water Resour. Res.*, 1997, **33**(1), 123–136.

21 A. I. Packman, M. Salehin and M. Zaramella, Hyporheic Exchange with Gravel Beds: Basic Hydrodynamic Interactions and Bedform-Induced Advective Flows, *J. Hydraul. Eng.*, 2004, **130**(7), 647–656.

22 A. Fox, F. Boano and S. Arnon, Impact of losing and gaining streamflow conditions on hyporheic exchange fluxes induced by dune-shaped bed forms, *Water Resour. Res.*, 2014, **50**(3), 1895–1907.

23 Z. Li, A. Sobek and M. Radke, Flume Experiments To Investigate the Environmental Fate of Pharmaceuticals and Their Transformation Products in Streams, *Environ. Sci. Technol.*, 2015, **49**(10), 6009–6017.

24 U. Kunkel and M. Radke, Biodegradation of Acidic Pharmaceuticals in Bed Sediments: Insight from a Laboratory Experiment, *Environ. Sci. Technol.*, 2008, **42**(19), 7273–7279.

25 G. Pinay, S. Peiffer, J.-R. De Dreuzy, S. Krause, D. M. Hannah, J. H. Fleckenstein, M. Sebilo, K. Bishop and L. Hubert-Moy, Upscaling Nitrogen Removal Capacity from Local Hotspots to Low Stream Orders' Drainage Basins, *Ecosystems*, 2015, **18**(6), 1101–1120.

 This journal is © The Royal Society of Chemistry 2019

Open Access Article. Published on 17 October 2019. Downloaded on 1/15/2026 12:16:42 AM.
This article is licensed under a Creative Commons Attribution 3.0 Unported Licence.

26 S. Krause, J. Lewandowski, N. B. Grimm, D. M. Hannah, G. Pinay, K. McDonald, E. Martí, A. Argerich, L. Pfister, J. Klaus, T. Battin, S. T. Larned, J. Schelker, J. Fleckenstein, C. Schmidt, M. O. Rivett, G. Watts, F. Sabater, A. Sorolla and V. Turk, Ecohydrological interfaces as hot spots of ecosystem processes, *Water Resour. Res.*, 2017, **53**(8), 6359–6376.

27 F. Boano, J. W. Harvey, A. Marion, A. I. Packman, R. Revelli, L. Ridolfi and A. Wörman, Hyporheic flow and transport processes: Mechanisms, models, and biogeochemical implications, *Rev. Geophys.*, 2014, **52**(4), 603–679.

28 J. P. Zarnetske, R. Haggerty, S. M. Wondzell, V. A. Bokil and R. González-Pinzón, Coupled transport and reaction kinetics control the nitrate source-sink function of hyporheic zones, *Water Resour. Res.*, 2012, **48**(11), W11508.

29 J. L. Schaper, M. Posselt, J. L. McCallum, E. W. Banks, A. Hoehne, K. Meinikmann, M. A. Shanafield, O. Batelaan and J. Lewandowski, Hyporheic Exchange Controls Fate of Trace Organic Compounds in an Urban Stream, *Environ. Sci. Technol.*, 2018, **52**(21), 12285–12294.

30 J. Schaper, M. Posselt, C. Bouchez, A. Jaeger, G. Nützmann, A. Putschew, G. Singer and J. Lewandowski, Fate of trace organic compounds in the hyporheic zone: influence of retardation, the benthic bio-layer and organic carbon, *Environ. Sci. Technol.*, 2019, **53**(8), 4224–4234.

31 J. P. Zarnetske, R. Haggerty, S. M. Wondzell and M. A. Baker, Dynamics of nitrate production and removal as a function of residence time in the hyporheic zone, *J. Geophys. Res.: Biogeosci.*, 2011, **116**(G1), G01025.

32 E. T. Hester, K. I. Young and M. A. Widdowson, Mixing of surface and groundwater induced by riverbed dunes: Implications for hyporheic zone definitions and pollutant reactions, *Water Resour. Res.*, 2013, **49**(9), 5221–5237.

33 L. B. Stadler, J. Delgado Vela, S. Jain, G. J. Dick and N. G. Love, Elucidating the impact of microbial community biodiversity on pharmaceutical biotransformation during wastewater treatment, *Microb. Biotechnol.*, 2018, **11**(6), 995–1007.

34 D. R. Johnson, D. E. Helbling, T. K. Lee, J. Park, K. Fenner, H. P. Kohler and M. Ackermann, Association of biodiversity with the rates of micropollutant biotransformations among full-scale wastewater treatment plant communities, *Appl. Environ. Microbiol.*, 2015, **81**(2), 666–675.

35 M. Jekel, W. Dott, A. Bergmann, U. Dunnbier, R. Gnirss, B. Haist-Gulde, G. Hamscher, M. Letzel, T. Licha, S. Lyko, U. Miehe, F. Sacher, M. Scheurer, C. K. Schmidt, T. Reemtsma and A. S. Ruhl, Selection of organic process and source indicator substances for the anthropogenically influenced water cycle, *Chemosphere*, 2015, **125**, 155–167.

36 I. J. Buerge, H.-R. Buser, M. Kahle, M. D. Müller and T. Poiger, Ubiquitous Occurrence of the Artificial Sweetener Acesulfame in the Aquatic Environment: An Ideal Chemical Marker of Domestic Wastewater in Groundwater, *Environ. Sci. Technol.*, 2009, **43**(12), 4381–4385.

37 S. Kahl, S. Kleinsteuber, J. Nivala, M. van Afferden and T. Reemtsma, Emerging Biodegradation of the Previously Persistent Artificial Sweetener Acesulfame in Biological Wastewater Treatment, *Environ. Sci. Technol.*, 2018, **52**(5), 2717–2725.

38 M. Posselt, A. Jaeger, J. L. Schaper, M. Radke and J. P. Benskin, Determination of polar organic micropollutants in surface and pore water by high-resolution sampling-direct injection-ultra high performance liquid chromatography-tandem mass spectrometry, *Environ. Sci.: Processes Impacts*, 2018, **20**, 1716–1727.

39 R. I. Griffiths, A. S. Whiteley, A. G. O'Donnell and M. J. Bailey, Rapid method for coextraction of DNA and RNA from natural environments for analysis of ribosomal DNA- and rRNA-based microbial community composition, *Appl. Environ. Microbiol.*, 2000, **66**(12), 5488–5491.

40 M. Morawe, H. Hoeke, D. K. Wissenbach, G. Lentendu, T. Wubet, E. Kröber and S. Kolb, Acidotolerant Bacteria and Fungi as a Sink of Methanol-Derived Carbon in a Deciduous Forest Soil, *Front. Microbiol.*, 2017, **8**, 1361.

41 A. Zaprasis, Y. J. Liu, S. J. Liu, H. L. Drake and M. A. Horn, Abundance of novel and diverse tfdA-like genes, encoding putative phenoxyalkanoic acid herbicide-degrading dioxygenases, in soil, *Appl. Environ. Microbiol.*, 2010, **76**(1), 119–128.

42 N. Weithmann, A. R. Weig and R. Freitag, Process parameters and changes in the microbial community patterns during the first 240 days of an agricultural energy crop digester, *AMB Express*, 2016, **6**(1), 53.

43 R Development Core Team, *R: A language and environment for statistical computing*, R Foundation for Statistical Computing, Vienna, Austria, 2010.

44 J. Oksanen, F. G. Blanchet, R. Kindt, P. Legendre, P. R. Minchin, R. B. O'Hara, G. L. Simpson, P. Solymos, M. H. H. Stevens and H. Wagner, *Vegan: Community Ecology Package. R*, 2014.

45 P. J. McMurdie and S. Holmes, phyloseq: An R Package for Reproducible Interactive Analysis and Graphics of Microbiome Census Data, *PLoS One*, 2013, **8**(4), e61217.

46 M. Mutz, E. Kalbus and S. Meinecke, Effect of instream wood on vertical water flux in low-energy sand bed flume experiments, *Water Resour. Res.*, 2007, **43**(10), W10424.

47 A. E. Magurran, *Measuring Biological Diversity*, Wiley, 2004.

48 F. Bonk, D. Popp, H. Harms and F. Centler, PCR-based quantification of taxa-specific abundances in microbial communities: Quantifying and avoiding common pitfalls, *J. Microbiol. Methods*, 2018, **153**, 139–147.

49 D. Tonina and J. M. Buffington, Hyporheic exchange in gravel bed rivers with pool-riffle morphology: Laboratory experiments and three-dimensional modeling, *Water Resour. Res.*, 2007, **43**(1), W01421.

50 M. B. Cardenas and J. L. Wilson, Hydrodynamics of coupled flow above and below a sediment–water interface with triangular bedforms, *Adv. Water Resour.*, 2007, **30**(3), 301–313.

51 European_Commission, Regulation (EC) No. 1907/2006 of the European Parliament and of the Council of 18 December 2006 concerning the Registration, Evaluation,

Open Access Article. Published on 17 October 2019. Downloaded on 1/15/2026 12:16:42 AM.
This article is licensed under a Creative Commons Attribution 3.0 Unported Licence.

Authorisation and Restriction of Chemicals (REACH), establishing a European Chemicals Agency, amending Directive 1999/45/EC and repealing Council Regulation (EEC) No. 793/93 and Commission Regulation (EC) No. 1488/94 as well as Council Directive 76/769/EEC and Commission Directives 91/155/EEC, 93/67/EEC, 93/105/EC and 2000/21/EC, in 2006.

52 J. H. Writer, R. C. Antweiler, I. Ferrer, J. N. Ryan and E. M. Thurman, In-Stream Attenuation of Neuro-Active Pharmaceuticals and Their Metabolites, *Environ. Sci. Technol.*, 2013, **47**(17), 9781–9790.

53 V. Acuña, D. von Schiller, M. J. García-Galán, S. Rodríguez-Mozaz, L. Corominas, M. Petrovic, M. Poch, D. Barceló and S. Sabater, Occurrence and in-stream attenuation of wastewater-derived pharmaceuticals in Iberian rivers, *Sci. Total Environ.*, 2015, **503–504**, 133–141.

54 Z. Li, A. Sobek and M. Radke, Fate of Pharmaceuticals and Their Transformation Products in Four Small European Rivers Receiving Treated Wastewater, *Environ. Sci. Technol.*, 2016, **50**(11), 5614–5621.

55 A. de Wilt, Y. He, N. Sutton, A. Langenhoff and H. Rijnaarts, Sorption and biodegradation of six pharmaceutically active compounds under four different redox conditions, *Chemosphere*, 2018, **193**, 811–819.

56 F. I. Hai, X. Li, W. E. Price and L. D. Nghiem, Removal of carbamazepine and sulfamethoxazole by MBR under anoxic and aerobic conditions, *Bioresour. Technol.*, 2011, **102**(22), 10386–10390.

57 J. R. Thelusmond, T. J. Strathmann and A. M. Cupples, Carbamazepine, triclocarban and triclosan biodegradation and the phylotypes and functional genes associated with xenobiotic degradation in four agricultural soils, *Sci. Total Environ.*, 2019, **657**, 1138–1149.

58 F. Liu, A. H. Nielsen and J. Vollertsen, Sorption and Degradation Potential of Pharmaceuticals in Sediments from a Stormwater Retention Pond, *Water*, 2019, **11**(3), 526.

59 Z. Gan, H. Sun, R. Wang, H. Hu, P. Zhang and X. Ren, Transformation of acesulfame in water under natural sunlight: Joint effect of photolysis and biodegradation, *Water Res.*, 2014, **64**, 113–122.

60 V. Martínez-Hernández, R. Meffe, S. Herrera, E. Arranz and I. de Bustamante, Sorption/desorption of non-hydrophobic and ionisable pharmaceutical and personal care products from reclaimed water onto/from a natural sediment, *Sci. Total Environ.*, 2014, **472**, 273–281.

61 H. C. Tülp, K. Fenner, R. P. Schwarzenbach and K.-U. Goss, pH-Dependent Sorption of Acidic Organic Chemicals to Soil Organic Matter, *Environ. Sci. Technol.*, 2009, **43**(24), 9189–9195.

62 F. R. Storck, C. Skark, F. Remmler and H.-J. Brauch, Environmental fate and behavior of acesulfame in laboratory experiments, *Water Sci. Technol.*, 2016, **74**(12), 2832–2842.

63 D. Yuan, H. Wang, Y. An, X. Guo and L. He, Insight into the binding properties of carbamazepine onto dissolved organic matter using spectroscopic techniques during grassy swale treatment, *Ecotoxicol. Environ. Saf.*, 2019, **173**, 444–451.

64 OECD, Test No. 106, *Adsorption–Desorption Using a Batch Equilibrium Method*, 2000.

65 M. Loreau, S. Naeem, P. Inchausti, J. Bengtsson, J. P. Grime, A. Hector, D. U. Hooper, M. A. Huston, D. Raffaelli, B. Schmid, D. Tilman and D. A. Wardle, Biodiversity and Ecosystem Functioning: Current Knowledge and Future Challenges, *Science*, 2001, **294**(5543), 804–808.

66 S. Castronovo, A. Wick, M. Scheurer, K. Nodler, M. Schulz and T. A. Ternes, Biodegradation of the artificial sweetener acesulfame in biological wastewater treatment and sandfilters, *Water Res.*, 2017, **110**, 342–353.

67 V. Burke, J. Greskowiak, T. Asmuß, R. Bremermann, T. Taute and G. Massmann, Temperature dependent redox zonation and attenuation of wastewater-derived organic micropollutants in the hyporheic zone, *Sci. Total Environ.*, 2014, **482–483**, 53–61.

68 L. Bardini, F. Boano, M. B. Cardenas, R. Revelli and L. Ridolfi, Nutrient cycling in bedform induced hyporheic zones, *Geochim. Cosmochim. Acta*, 2012, **84**, 47–61.

69 A. J. Boulton, S. Findlay, P. Marmonier, E. H. Stanley and H. M. Valett, The functional significance of the hyporheic zone in streams and rivers, *Annu. Rev. Ecol. Syst.*, 1998, **29**(1), 59–81.

 This journal is © The Royal Society of Chemistry 2019